

THESIS FOR THE DEGREE OF LICENTIATE OF ENGINEERING

**Mixed Effects Modelling and Optimal Design of
TNF α Response in LPS Challenge Studies**

Methods and Applications in Drug Discovery

Julia Larsson

Department of Mathematical Sciences
Division of Applied Mathematics and Statistics
Chalmers University of Technology and University of Gothenburg
Göteborg, Sweden 2021

Mixed Effects Modelling and Optimal Design of $\text{TNF}\alpha$ Response in LPS Challenge Studies
Methods and Applications in Drug Discovery
Julia Larsson

© Julia Larsson, 2021

Department of Mathematical Sciences
Division of Applied Mathematics and Statistics
Chalmers University of Technology and University of Gothenburg
SE-412 96 Göteborg
Sweden
Telephone +46 (0)31 772 1000

Typeset with \LaTeX
Printed by Chalmers digitaltryck
Göteborg, Sweden 2021

Mixed Effects Modelling and Optimal Design of $\text{TNF}\alpha$ Response in LPS Challenge Studies

Methods and Applications in Drug Discovery

Julia Larsson

Department of Mathematical Sciences
Division of Applied Mathematics and Statistics
Chalmers University of Technology and University of Gothenburg

Abstract

“Endotoxin and mycoplasma are Nature’s darkest secrets. If they are ever solved, Hell itself will open.” – Lewis Thomas ¹

Endotoxin, or lipopolysaccharides (LPS), are heterogeneous components from the cell wall of Gram-Negative bacteria and a common challenger in the field of drug discovery. In challenge studies a system is provoked by a challenger, such as LPS, which is a commonly used design when studying respiratory and immune-mediated diseases. Unfortunately, LPS challenge experiments with the purpose of determining the inhibiting effect of a drug on a biomarker, such as tumour necrosis factor alpha ($\text{TNF}\alpha$), gives complex data from which it is difficult to determine the drug effect. This thesis is based on three papers and focuses on the complexity of $\text{TNF}\alpha$ response data from LPS challenge studies and how mathematical tools can simplify the estimation of the pharmacodynamic effect of the drug.

The first paper presents a second-generation $\text{TNF}\alpha$ turnover model able to capture $\text{TNF}\alpha$ response data from an extensive data set, using the non-linear mixed effects (NLME) modelling framework. The second paper uses the developed second-generation model for improvement of the experimental design in LPS challenge studies, in order to make the $\text{TNF}\alpha$ response data from LPS challenge studies as informative as possible. The third and last paper describes a user-friendly software package in Mathematica for estimation and evaluation of NLME models, called `NLMEModeling`, where the dynamical systems can be described either as ordinary or stochastic differential equations.

Keywords: Tumour necrosis factor alpha ($\text{TNF}\alpha$), lipopolysaccharides (LPS), pharmacokinetics and pharmacodynamics (PK/PD), non-linear mixed effects modelling (NLME), optimal design

¹K. Brigham, editor. *Endotoxin and the lungs*, volume 77. Marcel Dekker Inc., New York, 1994. ISBN 0-8247-9222-X.

List of publications

This thesis is based on the work represented by the following papers:

- I. **J. Larsson**, E. Hoppe, M. Gautrois, M. Cvijovic and M. Jirstrand. Second-generation $\text{TNF}\alpha$ turnover model for improved analysis of test compound interventions in LPS challenge studies. *European Journal of Pharmaceutical Sciences*. 165:105937, 2021. doi: 10.1016/j.ejps.2021.105937
- II. **J. Larsson**, E. Hoppe, M. Gautrois, M. Cvijovic and M. Jirstrand. Optimizing study design in LPS challenge studies for quantifying drug induced inhibition of $\text{TNF}\alpha$ response: Did we miss the prime time? *Manuscript*.
- III. J. Leander, J. Almquist, A. Johnning, **J. Larsson** and M. Jirstrand. NLMEM-odeling: A Wolfram Mathematica Package for Nonlinear Mixed Effects Modeling of Dynamical Systems. *arXiv preprint: arXiv:2011.06879 [stat.CO]*, 2020. ²

²A peer-reviewed conference paper (short version of the preprint) has been presented at SYSID 2021: J. Leander, J. Almquist, A. Johnning, J. Larsson and M. Jirstrand. Nonlinear Mixed Effects Modeling of Deterministic and Stochastic Dynamical Systems in Wolfram Mathematica. *In Proceedings of the 19th IFAC Symposium on System Identification (SYSID)*, 2021.

Author contributions

- I. Refined and analysed the existing model, performed all computational work – including the implementation and evaluation of the parameter estimation in Mathematica, evaluated the results by comparing it with previously published results, interpreted and validated the results from a biological point of view, created all figures and tables, drafted and edited the manuscript.
- II. Summarised the literature for an overview of the research field, performed all computational work – including implementation of model simulations in Mathematica and optimal design in R, evaluated the results by comparing it with previously published results, interpreted and validated the results from a biological and practical point of view, created all figures and tables, drafted and edited the manuscript.
- III. Code developing for improvements of model evaluation tools in `NLMEModeling` package, edited the manuscript.

Acknowledgements

I want to thank my supervisor Mats Jirstrand for his guidance, his never-ending optimism and for giving me the freedom to form my own research throughout the years. I also want to thank my supervisor Marija Cvijovic for her constant support and wise words when I needed them the most. I've grown so much, professionally and personally, with you two by my side. I also want to thank Johan Gabrielsson and Edmund Hoppe for their expertise within the field of pharmacokinetic/pharmacodynamic modelling and pharmacology, respectively, as well as for their great enthusiasm. Especially, I want to thank Grünenthal GmbH for enabling this project financially.

There are also those who have helped me a lot in both various projects and in my PhD studies in general without any obligation to do so, but who gladly did anyway. Thank you Jacob for our great scientific discussions and your constant encouragement, thank you Felix for sharing your experience with me from when you had this project, and thank you Anna for non-judgmentally answering my basic programming questions or just listening to me raging about how much I hate tables in Mathematica.

Those who have meant a lot to me from a more social perspective are my fellow PhD colleagues from FCC – Marcus, Viktor and Mattias – and the members of Cvijovic Lab – Barbara, Linnea, Patrick, Svenja, Sebastian, Johannes and Niek. Thank you for all the weird discussions, the after-works, and laughter's over the years. Thank you also Gabrijela, Gustav, Ulrika and Johanna for all interesting chats in the lunch room or in the corridors.

Lastly, I want to thank my friends and family, especially my parents Tony and Maria as well as my partner David. Without your support I would have never made it through the hardships I have faced. I love you all so much.

Julia Larsson,
Gothenburg, August 2021

Contents

Abstract	iii
List of publications	v
Acknowledgements	vii
Contents	ix
1 Introduction	1
1.1 Background	1
1.2 Problem Formulation	2
1.3 Thesis Structure	3
2 Methods	5
2.1 Pharmacokinetic/Pharmacodynamic Modelling	5
2.2 Non-Linear Mixed Effects Modelling	11
2.3 Estimating Model Parameters	14
2.4 Model Evaluation Tools	17
2.5 Optimal Design	21

3	Summary of Papers	27
4	Outlook	31
	Bibliography	35
	Papers I-III	

1 Introduction

1.1 Background

Mathematical modelling within drug discovery is an expanding field and an important tool for analysing biological phenomena [1]. By creating a mathematical model with the ability to describe experimental data, for example time-series data of a drug or biomarker of interest, it opens up new possibilities of how we can study the problem at hand. The model can be used to simulate data under circumstances that are not feasible from an economical or ethical stand-point, to better estimate system parameters for more accurate results, as well as to plan future studies to be as informative as possible [1, 2, 3]. For example, mathematical modelling serves as a good supplement to animal testing in pre-clinical studies, where insight from both a mathematical and pharmacological perspective is crucial for a successful outcome [3, 4].

Mathematical modelling becomes especially important when analysing data from challenge studies. In a challenge study the effect of a drug is tested on a system provoked by a challenger, and is a commonly used study design in respiratory and immune-mediated diseases [1]. A well-known challenger is the lipopolysaccharide (LPS), which are large molecules from the cell wall of Gram-Negative bacteria [5]. LPS challenge studies are used when studying the ability of a drug to inhibit biomarkers related to immuno-response, such as interleukins (IL), nitric oxides (NO), or tumour necrosis factor alpha ($\text{TNF}\alpha$) which this thesis will focus on [6]. A problem with LPS challenge studies is that the distinction between the inhibitory effect of the drug from the stimulatory effect of LPS in immuno-response data is complicated. Firstly, neither the $\text{TNF}\alpha$ response in absence of LPS, nor the LPS concentrations, are measurable *in vivo*. Secondly, $\text{TNF}\alpha$ response is highly variable between individuals, as a consequence of the animals reacting differently to the LPS provocation [7, 8]. It thus exists a need to accurately describe immuno-response data from LPS

challenge studies, as well as optimise the design of experiments to make the resulting data more informative, for more robust and reliable estimates of the inhibitory effect of the drug.

These research questions have been addressed in this thesis. In Paper I we construct a mathematical model for prediction and analysis of $\text{TNF}\alpha$ after LPS challenge doses and drug interventions, using an extensive data set. We base our model on a previously published model by our group [9] and the aim with the work is to produce a framework of how to model $\text{TNF}\alpha$ response in LPS challenge studies *in vivo* and demonstrate its general applicability regardless of occasion or type of test compound. In Paper II we then use our model for optimisation of study design for future experiments. The goal with this work is to show how to optimise the planning of experiments to maximise the information in a limited data set, as well as provide guidelines to both modellers and experimentalists on how to study $\text{TNF}\alpha$ response data from LPS challenge studies. Lastly, in Paper III the Mathematica package `NLMEModeling` is described in detail, which have been used to construct, estimate, and validate the chosen model.

1.2 Problem Formulation

The overall aim with this thesis is to better understand *in vivo* $\text{TNF}\alpha$ response data in pre-clinical LPS challenge studies, using mathematical modelling, and use that knowledge to improve the estimation of inhibiting drug effect. This is achieved by, firstly, in Paper I creating and evaluating a mathematical model describing $\text{TNF}\alpha$ response in Sprague-Dawley rats to retrieve reliable estimates of the drug effect. Secondly, in Paper II we use that model to optimise the study design of $\text{TNF}\alpha$ response to retrieve more informative data for future experiments. Lastly, in Paper III the different methodologies of parameter estimation, model simulations, and model evaluation is presented which gives a good insight of how the results have been retrieved.

1.3 Thesis Structure

Chapter 2 introduces relevant topics such as mathematical modelling, parameter estimation, model evaluation tools, and optimal study design, in order to fully appreciate the work done in the appended papers. Chapter 3 then summarises each paper and in Chapter 4 a brief outlook discussing future research is presented.

2 Methods

2.1 Pharmacokinetic/Pharmacodynamic Modelling

The term “mathematical modelling” can have different meaning depending on the context, but in this thesis the term is used interchangeably with pharmacokinetic and pharmacodynamic (PK/PD) modelling. PK/PD models are typically described using time-dependent ordinary differential equations (ODEs), and have their roots in compartmental modelling, enzyme kinetics, and chemical reaction equations [2, 10, 11]. Although the extension to stochastic differential equations (SDEs) has increased in popularity within the field of PK/PD modelling, this thesis will only consider PK/PD models using ODEs [12].

The pharmacokinetics of a drug can be described as “what the body does to the drug”, while the pharmacodynamics of a drug can be described as “what the drug does to the body”, where PK/PD models are mathematical representations of the phenomena. PK models concerns how the drug concentration changes over time and how it travels from administration route to its active site, for example how an oral dose travels to the blood circulation via the gut (Fig. 2.1). The PD model on the other hand describes the time course of the drug effect on response, where the response could be biomarkers and receptors, or functional responses such blood pressure and heart rate [1]. In this simplistic way of describing a complex biological system one can extract the key characteristics of the system, for example the *clearance* (how fast the drug is eliminated), the *bioavailability* (the fraction of the drug that reaches the systemic circulation intact), and the *potency* (usually quantified by the drug concentration required to obtain 50% treatment effect, for example 50% inhibition of $\text{TNF}\alpha$ response).

In the field of PK/PD modelling, the model building process is characterised by adding and connecting several models or compartments, that serve as building blocks with its own specific effect on the model as a whole. A simple model could be built with only a few components while a more complex model

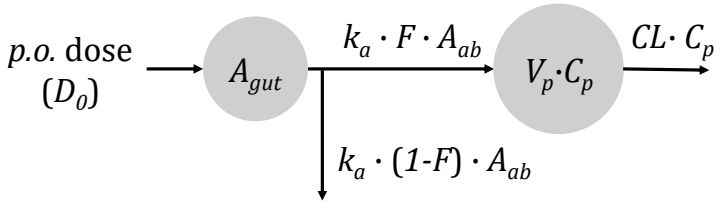


Figure 2.1: A typical two-compartmental model describing how a *per oral* dose D_0 enters the blood circulation via the gut. Here A_{gut} is the amount of drug in the gut and C_p the drug concentration in plasma. The parameters are the absorption rate k_a , the bioavailability F , the volume of distribution in plasma V_p , and clearance CL .

would use several building blocks connected to each other, where the model complexity is dependent of the biological system to be studied and the richness of the data. Examples of these building blocks are biophase distribution models, turnover models, direct effect models or signal transduction models. Only a handful of the available building blocks are presented in this thesis, and for a review of the most common building blocks, see [2].

2.1.1 Compartmental and Non-compartmental Modelling

PK/PD models can be constructed using either compartmental or non-compartmental modelling, where compartmental modelling is an established technique for building models using interconnected compartments while non-compartmental modelling more focuses on the mathematical expressions characterising the different types of response. Compartments can be described as containers containing an amount or concentration of a substance (such as a drug or response), where a compartment could correspond to a physically existing entity in the body (gut or plasma) or a more abstract entity (a central or peripheral compartment) [10, 13]. Each compartment is assumed to be well-mixed, meaning that the amount or concentration of substance entering the compartment is instantaneously homogeneously distributed within the compartment [14]. In compartmental modelling these containers are connected with different types of flows: External in- and outflow corresponding to a substance entering or leaving the system, mass transfer of a substance from one compartment to another, and control signals where the presence of a substance affects the production or elimination of another substance through either stimulation or inhibition. Note that the substance exerting the control action is not affected itself.

To demonstrate, the PK model visualised in Fig. 2.1 would translate to a system

of ODEs described as

$$\begin{aligned} \frac{dA_{gut}}{dt} &= -k_a \cdot A_{gut}, & A_{gut}(0) &= D_0 \\ V_p \cdot \frac{dC_p}{dt} &= k_a \cdot F \cdot A_{gut} - CL \cdot C_p, & C_p(0) &= 0 \end{aligned} \quad (2.1)$$

where A_{gut} is the amount of drug in the gut compartment and C_p is the drug concentration in the plasma compartment, respectively. The parameters are the absorption rate constant k_a , the bioavailability F , the volume of distribution in the plasma compartment V_p , the clearance CL , and the initial drug dose D_0 . The flows in this model would be the inflow of drug to the gut compartment, the mass transfer from the gut to the plasma compartment, and the outflow from the plasma compartment. For more examples on simple compartmental models, see [1].

The same PK model can be described using non-compartmental modelling, where the observed system is instead viewed as a sum of exponentials rather than a flow between compartments. The system would in this case be described as an uncoupled system of ODEs

$$\begin{aligned} \frac{dx_1}{dt} &= -K_a \cdot x_1, & x_1(0) &= A \\ \frac{dx_2}{dt} &= -K_e \cdot x_2, & x_2(0) &= A \\ C(t) &= x_1(t) - x_2(t) \end{aligned} \quad (2.2)$$

where the variables x_1 and x_2 do not correspond to any compartment but together defines the observed concentration in plasma C . The parameters here are the absorption rate constant K_a , the elimination rate constant K_e and the concentration constant A . This setting is preferred if the data is unable to distinguish CL from V_p , but comes with several drawbacks. Firstly, the information concerning D_0 is not used. Secondly, since equation (2.2) is not described as a transfer of mass, the concentration C could be negative which would have otherwise been impossible for a model built by interconnected compartments. Lastly, and maybe most importantly, equation (2.2) lacks biological interpretation in comparison to equation (2.1). Therefore, compartmental modelling is in many cases the superior, but non-compartmental modelling can prove to be useful if the number of parameters needs to be reduced.

2.1.2 Turnover Models and Challenge Models

Turnover models, or indirect response models, describe how a drug or treatment can perturb a system response in steady-state, and are often based on biological phenomena with parameters that have a physiological meaning. The drug effect could either be reversible (enzyme inhibited by drug where the drug is eliminated with time) or irreversible (killing of bacteria or tumour cells with antibiotics or chemotherapy, respectively), where in this thesis only reversible effects are considered. The rate of change of the response can be described as

$$\frac{dR}{dt} = k_{in} - k_{out}R(t), \quad R(0) = R_0 \quad (2.3)$$

where $R(t)$ is the response, k_{in} the zero-order input, k_{out} the first-order output, and R_0 the baseline response. In absence of a drug the response is commonly in steady-state, according to the equation:

$$\frac{dR}{dt} = k_{in} - k_{out}R(t) = 0 \quad \Rightarrow \quad R_0 = \frac{k_{in}}{k_{out}} \quad (2.4)$$

From this the system can be perturbed with a drug effect that is either stimulatory or inhibitory. Stimulation and inhibition are commonly defined as

$$S(C) = 1 + \frac{S_{max} \cdot C^n}{SC_{50}^n + C^n} \quad \text{or} \quad I(C) = 1 - \frac{I_{max} \cdot C^n}{IC_{50}^n + C^n} \quad (2.5)$$

where C is the treatment concentration, $S_{max} > 0$ and $0 < I_{max} \leq 1$ are the maximal stimulatory or inhibitory effect, SC_{50} and IC_{50} are the drug concentration where 50% stimulation or inhibition is achieved (potency), and n is the Hill coefficient. In the case of indirect responses, the expressions in (2.5) act multiplicative on either the input k_{in} or output k_{out} in (2.3) that in total could give four different perturbations of the system, see Fig. 2.2.

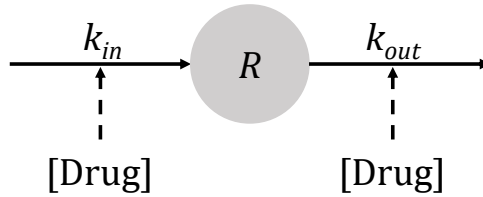


Figure 2.2: Schematic representation of an indirect reversible response model, where the drug effect could be either stimulatory or inhibitory.

Although all four models have their similarities and differences, insight in how the drug affects the biological system at hand could be very helpful in the model selection. If the drug, for instance, inhibits an enzyme it is desirable to know how the enzyme indirectly affects the response, such that a distinction between for example inhibition on input from stimulation of output can be made. For more examples of turnover models, reversible or irreversible, as well as examples of both direct and indirect response models, see [1].

In some cases the input k_{in} in (2.3) is not necessarily constant in time, namely not a zero-order input, which in turn creates a time-varying baseline. Challenge studies in general, and $\text{TNF}\alpha$ response in LPS challenge studies in particular, are examples of systems with a time-varying baseline. Since the $\text{TNF}\alpha$ response in absence of LPS is immeasurable, it would correspond to a baseline response of $R_0 = 0$. However, when a challenger is added to the system it creates a stimulation of response that can be described by

$$\frac{dR}{dt} = S(C) - k_{out}R(t), \quad R(0) = 0 \text{ and } S(C) = \frac{S_{max} \cdot C^n}{SC_{50}^n + C^n} \quad (2.6)$$

where all terms are defined in the equations (2.3) and (2.5) above. If an inhibiting drug is simultaneously given with the challenger, either an inhibition function can act multiplicative on the input or a stimulation function can act multiplicative on the output, once again dependent on the biological effect of the drug on the system. For more examples concerning challenge models, see [15].

2.1.3 Biophase Models and Transit Compartment Models

Another common trait of $\text{TNF}\alpha$ response in LPS challenge studies is that the response is time-delayed, resulting in an $\text{TNF}\alpha$ peak response 1-2h after LPS administration [16, 17]. To take into account the time-delay, biophase models or signal transduction models can be used, depending on the duration of the delay. The biophase model introduces a theoretical effect compartment separate from the plasma compartment, with the idea that a negligible amount of drug or challenge enters the effect compartment where the actual effect on response occurs. In this way a small time-delay is created, while the profile of the drug or challenge in the plasma compartment remains unchanged [2]. The dynamics in the effect compartment is modelled as

$$\frac{dC_e}{dt} = k_{1e}C_p - k_{0e}C_e \quad (2.7)$$

where C_e is the concentration of drug or challenge in the arbitrary effect compartment, C_p is the concentration in the plasma compartment, and k_{1e} and k_{0e} are first-order distribution rate constants. The biophase model is also shown conceptually in Fig. 2.3A.

If an even longer time-delay is required, the transit compartment model is preferred. The basic idea with the transit compartment model is that the flow is delayed by bypassing a chain of transit compartments that slows down the process. The flow between compartments is governed by the mean transit time τ , and is modelled as

$$\begin{aligned} \frac{dS_1}{dt} &= In - \frac{1}{\tau}S_1 \\ \frac{dS_2}{dt} &= \frac{1}{\tau}(S_1 - S_2) \\ &\vdots \\ \frac{dS_N}{dt} &= \frac{1}{\tau}(S_{N-1} - S_N) \end{aligned} \quad (2.8)$$

where In is an arbitrary input and S_1, S_2, \dots, S_N is the N number of transit compartments, see also Fig. 2.3B. For methods determining the number of transit compartments, see [18]. The transit compartments can be compared with a biological signalling cascade that in turn leads to response, but each

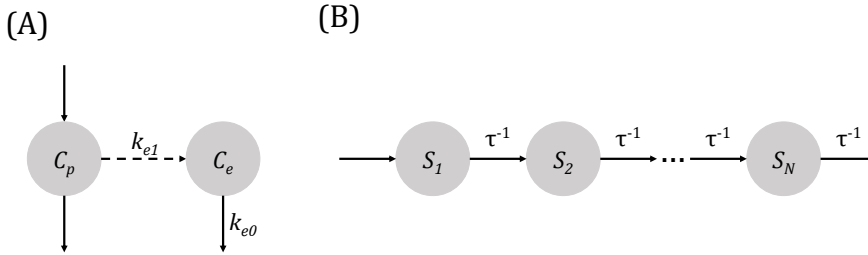


Figure 2.3: (A) Schematic representation of a biophase model, where the production and elimination of the drug or challenger in the plasma compartment (C_p) are denoted with solid arrows, the diffusion from the plasma compartment to the effect compartment is denoted with a dashed arrow, and the elimination of drug or challenger in the effect compartment (C_e) is denoted a solid arrow. (B) Schematic representation of the signal transduction model with transit compartments S_1, S_2, \dots, S_N and mean transit time τ .

transit compartment does not necessarily need to correspond to physical compartments of the cascade [2, 18]. The transit compartment model can also be interpreted as a simple signal transduction process, although more complex transduction processes are usually more common.

2.2 Non-Linear Mixed Effects Modelling

In section 2.1 some of the most common building blocks are presented and in turn how they can be connected to create a PK/PD model. However, although the PK/PD models are able to capture the key characteristics seen in data, they lack the ability to describe the different sources of variability in a data set. Since a drug or treatment is often tested on several test subjects, there will exist an inter-individual variability based on the fact that every individual responds differently to a provocation or treatment. Therefore, the ODEs presented in section 2.1 are extended to non-linear mixed effects (NLME) models, that allow for different descriptions of the inter-individual variability, as well as the observation error [19].

Consider a state space model with continuous time dynamics and discrete time observations that consists of four parts; a system of first order ODEs, an initial condition, an observation model, and an observation error model:

$$\begin{aligned}
\frac{d\mathbf{x}}{dt} &= \mathbf{f}(\mathbf{x}, \mathbf{u}, t, \boldsymbol{\theta}), & \mathbf{x}(t_0) &= \mathbf{x}_0(\boldsymbol{\theta}) \\
\mathbf{y}_j &= \mathbf{g}(\mathbf{x}(t_j), \mathbf{u}(t_j), t_j, \boldsymbol{\theta}) + \mathbf{e}(t_j) \\
\mathbf{e}(t_j) &\sim \mathcal{N}(0, \boldsymbol{\Sigma}(\mathbf{x}(t_j), \mathbf{u}(t_j), t_j, \boldsymbol{\theta}))
\end{aligned} \tag{2.9}$$

Here \mathbf{x} is a vector of state variables, \mathbf{y}_j are the observations for each time point j , t is the continuous time and t_j the sampling time points, \mathbf{u} is a vector of system inputs (such as different dosing regimens), $\boldsymbol{\theta}$ is a vector of population parameters, and $\mathbf{e}(t_j)$ is the independent normally distributed observation error with zero mean and covariance matrix $\boldsymbol{\Sigma}(\mathbf{x}(t_j), \mathbf{u}(t_j), t_j, \boldsymbol{\theta})$. For examples of different observation error models $\boldsymbol{\Sigma}$, see [20]. The function $\mathbf{f}(\mathbf{x}, \mathbf{u}, t, \boldsymbol{\theta})$ describes the dynamics of the system with initial condition $\mathbf{x}_0(\boldsymbol{\theta})$, for example the PK model presented in Eq. (2.1), while $\mathbf{g}(\mathbf{x}(t_j), \mathbf{u}(t_j), t_j, \boldsymbol{\theta})$ describes the observation model, for example the drug concentration in plasma.

Extending the general state space model to the NLME modelling framework yields

$$\begin{aligned}
\frac{d\mathbf{x}_i}{dt} &= \mathbf{f}(\mathbf{x}_i, \mathbf{u}_i, t, \boldsymbol{\phi}_i), & \mathbf{x}_i(t_0) &= \mathbf{x}_{i,0}(\boldsymbol{\phi}_i) \\
\mathbf{y}_{ij} &= \mathbf{g}(\mathbf{x}_i(t_{ij}), \mathbf{u}_i(t_{ij}), t_{ij}, \boldsymbol{\phi}_i) + \mathbf{e}_i(t_{ij}) \\
\mathbf{e}_i(t_{ij}) &\sim \mathcal{N}(0, \boldsymbol{\Sigma}(\mathbf{x}_i(t_{ij}), \mathbf{u}_i(t_{ij}), t_{ij}, \boldsymbol{\phi}_i))
\end{aligned} \tag{2.10}$$

where there are only two major differences compared to the original model: Firstly, an index $i = 1, \dots, N$ has been added to all parameters and variables except the continuous time t , meaning that Eq. (2.10) describes the dynamics of every individual i in the population. Secondly, the population parameter vector $\boldsymbol{\theta}$ (or equivalently the fixed effects vector) has been replaced by $\boldsymbol{\phi}_i$, which is a vector of parameters for each individual according to the relationship

$$\boldsymbol{\phi}_i = \boldsymbol{\phi}_i(\boldsymbol{\theta}, \mathbf{Z}_i, \boldsymbol{\eta}_i) \tag{2.11}$$

where $\boldsymbol{\theta}$ is a vector of fixed effects common for all individuals, \mathbf{Z}_i is a vector of known individual covariates (such as weight, age etc.), and $\boldsymbol{\eta}_i$ is a vector of random effects that are different for each individual. We assume $\boldsymbol{\eta}_i, i = 1, \dots, N$ are independent and follow a multivariate normal distribution accordingly

$$\boldsymbol{\eta}_i \sim \mathcal{N}(0, \boldsymbol{\Omega}) \quad (2.12)$$

where $\boldsymbol{\Omega}$ is the random effects covariance matrix of size $K \times K$, where K denotes the number of random effects parameters. The matrix is often assumed to be a diagonal matrix, although correlation between the diagonal elements is possible. The most common assumptions are that the parameters in ϕ_i are either normally distributed, log-normally distributed, or logit-normally distributed

$$\begin{aligned} \phi_{ip} &= \theta_p + \eta_{ik}, \text{ or} \\ \phi_{ip} &= \theta_p \exp^{\eta_{ik}}, \text{ or} \\ \phi_{ip} &= \frac{1}{1 + \exp(-(\theta_p + \eta_{ik}))} \\ \eta_{ik} &\sim \mathcal{N}(0, \omega_k^2) \end{aligned} \quad (2.13)$$

for the fixed effects parameter $\theta_p, p = 1, 2, \dots, P$ and random effects parameter η_{ik} with standard deviation $\omega_k, k = 1, 2, \dots, K$, and for each individual $i = 1, 2, \dots, N$. By describing the variability in data with both inter-individual variability and observation error (given that data is of population character), the observation error will decrease relative to the original system in Eq. (2.9) as well as increase the precision in the estimated parameters, at the cost that the model complexity increases.

As a last remark on the topic, one can add inter-occasion variability (or inter-study variability) to the NLME framework. Inter-occasion variability is required if there exist an apparent difference in the observations in a common population, where the experiments have been conducted at two different occasions [21]. Although there exist many ways to mathematically consider inter-occasion variability, only the simplest relationship is presented here

$$\theta_p = \sum_{m=1}^M \theta_{pm} \cdot \text{Study}_m \quad (2.14)$$

where Study_m is either 1 if the individuals are in study group $m = 1, 2, \dots, M$ and 0 else. For more examples of implementation of inter-occasion variability, see [21].

2.3 Estimating Model Parameters

After selecting a model structure that captures the key characteristics in a data set and adding inter-individual variability to the model, using the NLME modelling framework, the next step is to infer the model parameters from the experimental data. A common parameter estimation method is the maximum likelihood approach, where the goal is to find the parameter values such that, given a statistical model, the observed data is most probable. By defining a parametrised probabilistic model for the data and maximising the likelihood with respect to the parameters, a maximum likelihood parameter estimate can be found. However, for most NLME models the likelihood function lacks a closed-form solution and thus needs to be approximated, where the first-order conditional estimation (FOCE) approximation and stochastic approximation expectation maximization (SAEM) are two popular choices [22, 23]. In this section focus will be on the FOCE approximation of the likelihood function, as well as optimisation methods used in `NLMEModelling` [24].

2.3.1 Derivation of the Likelihood Function

The likelihood function is the joint probability distribution evaluated for a set of given experimental data viewed as a function of the model parameters. For a statistical model in general, given a data set \mathcal{D} and parameters θ , the likelihood can be defined as:

$$\mathcal{L}(\theta|\mathcal{D}) \triangleq p(\mathcal{D}|\theta) \quad (2.15)$$

For NLME models specifically the parameter inference becomes more complicated, since the random effects η_i are unobserved entities. To formulate the likelihood function removing the dependency of these unobserved entities, the joint distribution of the data and random effects are marginalised with respect to η_i , in order to get an expression of the likelihood that is only dependent of the model parameters θ , Ω , and Σ . After marginalisation with respect to η_i , assuming independence between individuals, the expression becomes

$$\mathcal{L}(\theta, \Sigma, \Omega|\mathcal{D}) = \prod_{i=1}^N \int p(\mathcal{D}_i, \eta_i|\theta, \Sigma, \Omega) d\eta_i \quad (2.16)$$

where $\mathcal{D}_i = \{\mathbf{d}_{i1}, \mathbf{d}_{i2}, \dots, \mathbf{d}_{in_i}\}$ is the collection of observations for individual $i = 1, 2, \dots, N$ and observations $j = 1, 2, \dots, n_i$, and $\mathcal{D} = \{\mathcal{D}_1, \mathcal{D}_2, \dots, \mathcal{D}_N\}$ represents the complete set of observations. If applying Bayes' theorem on the right hand side of Eq. (2.16), the expression becomes

$$\mathcal{L}(\boldsymbol{\theta}, \boldsymbol{\Sigma}, \boldsymbol{\Omega}|\mathcal{D}) = \prod_{i=1}^N \int p(\mathcal{D}_i|\boldsymbol{\theta}, \boldsymbol{\Sigma}, \boldsymbol{\Omega}, \boldsymbol{\eta}_i)p(\boldsymbol{\eta}_i|\boldsymbol{\theta}, \boldsymbol{\Sigma}, \boldsymbol{\Omega})d\boldsymbol{\eta}_i \quad (2.17)$$

and by noticing that $\boldsymbol{\eta}_i$ and $\boldsymbol{\theta}$, as well as $\boldsymbol{\eta}_i$ and $\boldsymbol{\Sigma}$, are conditionally independent given $\boldsymbol{\Omega}$, Eq. (2.17) is reduced to:

$$\mathcal{L}(\boldsymbol{\theta}, \boldsymbol{\Sigma}, \boldsymbol{\Omega}|\mathcal{D}) = \prod_{i=1}^N \int p(\mathcal{D}_i|\boldsymbol{\theta}, \boldsymbol{\Sigma}, \boldsymbol{\eta}_i)p(\boldsymbol{\eta}_i|\boldsymbol{\Omega})d\boldsymbol{\eta}_i \quad (2.18)$$

Since both the observations and random effects are assumed to be normally distributed, the right hand side can be rewritten using an individual joint log likelihood $l_i(\boldsymbol{\eta}_i)$

$$\mathcal{L}(\boldsymbol{\theta}, \boldsymbol{\Sigma}, \boldsymbol{\Omega}|\mathcal{D}) = \prod_{i=1}^N \int \exp(l_i(\boldsymbol{\eta}_i))d\boldsymbol{\eta}_i \quad (2.19)$$

where $l_i(\boldsymbol{\eta}_i)$ in turn becomes:

$$l_i(\boldsymbol{\eta}_i) = -\frac{1}{2} \sum_{j=1}^{n_i} (\boldsymbol{\varepsilon}_{ij}^T \boldsymbol{\Sigma}^{-1} \boldsymbol{\varepsilon}_{ij} + \log \det 2\pi \boldsymbol{\Sigma}) - \frac{1}{2} \boldsymbol{\eta}_i^T \boldsymbol{\Omega}^{-1} \boldsymbol{\eta}_i - \frac{1}{2} \log \det 2\pi \boldsymbol{\Omega} \quad (2.20)$$

Here $\boldsymbol{\varepsilon}_{ij}$ are the residual errors defined as

$$\begin{aligned}\varepsilon_{ij} &= \mathbf{d}_{ij} - \hat{\mathbf{y}}_{ij} \\ \hat{\mathbf{y}}_{ij} &= \mathbb{E}[\mathbf{y}_{ij} | \mathcal{D}_{i(j-1)}]\end{aligned}\tag{2.21}$$

and $\hat{\mathbf{y}}_{ij}$ is the predicted model output conditioned on the available information up to time point $t_{i(j-1)}$ ($\mathcal{D}_{i(j-1)} = \{\mathbf{d}_{i1}, \mathbf{d}_{i2}, \dots, \mathbf{d}_{i(j-1)}\}$). The integral in Eq. (2.19) with respect to $\boldsymbol{\eta}_i$ seldom has closed-form solutions. Therefore, the integral is approximated using a second-order Taylor expansion of l_i around the point $\boldsymbol{\eta}_i^*$ that maximises l_i , which often is referred to the Laplacian approximation [25]. This closed-form expression of the marginalisation yields the following approximate expression for the log-likelihood

$$\log L_L(\boldsymbol{\theta}, \boldsymbol{\Sigma}, \boldsymbol{\Omega} | \mathcal{D}) = \sum_{i=1}^N \left(l_i(\boldsymbol{\eta}_i^*) - \frac{1}{2} \log \det \frac{-\mathbf{H}_i(\boldsymbol{\eta}_i^*)}{2\pi} \right)\tag{2.22}$$

where the log-likelihood has the same maximum as the likelihood, since the logarithmic function is monotonically increasing. The matrix $\mathbf{H}_i(\boldsymbol{\eta}_i^*)$ is the Hessian of l_i evaluated at $\boldsymbol{\eta}_i^*$, and depending on the number of terms kept in an approximated expression of the Hessian, the Laplacian method (FOCE), or the FOCE with interaction (FOCEI) are obtained. For further information, see [26].

2.3.2 Gradient Based Optimization

The maximum likelihood estimate is obtained by maximising the approximate log-likelihood with respect to the model parameters

$$\boldsymbol{\Theta}^* = \underset{\boldsymbol{\Theta}}{\operatorname{argmax}} \log L_L\tag{2.23}$$

where $\boldsymbol{\Theta}$ denote the collection of parameters $\{\boldsymbol{\theta}, \boldsymbol{\Omega}, \boldsymbol{\Sigma}\}$. This can be achieved by, for example, using a gradient-based optimisation method called the Broyden-Fletcher-Goldfarb-Shanno (BFGS) algorithm [27]. The BFGS algorithm is a local optimisation method and belongs to the family of quasi-Newton methods. Specifically, it is an iterative algorithm for solving unconstrained nonlinear optimisation problems. In `NLMEModeling` described in Paper III, the gradient of the objective function is calculated using an exact method, instead of the

previous state-of-the-art solution relying on a finite difference approach. For a derivation of the exact gradients in `NLMEModeling`, see [26, 28]. To obtain the uncertainty in the estimated parameters, `NLMEModeling` uses the variance-covariance matrix of the estimated parameters, given by the negative inverse of the Hessian matrix at the optimum. Lastly, the point η_i^* , calculated given the optimal parameter values Θ^* , is the most likely random effects for each subject. These are referred to as the empirical Bayes estimates (EBEs).

2.4 Model Evaluation Tools

After constructing the model and finding the optimal parameter values, the next step is to evaluate how well the chosen model represents data. This is done by using different model evaluation tools for validation of the result. Model evaluation tools are mainly graphical methods used for data visualisation, inspection of model adequacy, and assumption testing [29]. There exist a whole toolbox of graphical methods validating specific model assumptions and properties, and using only one graphical method is seldom enough to get a good understanding of how well the model fits data. The graphical methods of interest, which also are my main contributions to Paper III, are discussed further below and for a complete list, see [30].

2.4.1 Empirical Bayes Estimates Based Diagnostics

Recall from section 2.3.2 that the point η_i^* , calculated given the optimal parameter values Θ^* , are referred to as the empirical Bayes estimates (EBEs). Although they might be optimal for the given model, it does not necessarily mean that the assumption that $\eta_i^* \sim \mathcal{N}(0, \Omega)$ is fulfilled for all individuals i (see section 2.2). The following three model evaluation tools examine if the assumption of normality is properly fulfilled, or if there exist unspecified dependencies between EBEs and other variables in the model. The purpose of each tool is illustrated using a PK model with two random effects parameters, where the corresponding EBEs for all individuals i and each random effects k are henceforth called η_{EBE}^k , $k = 1, 2$ (see Fig. 2.4).

The first validation tool checks if the elements in η_{EBE}^k truly are sampled from a normal distribution with standard deviation ω_k . This is done by calculating the η -shrinkage, which is a measure used for comparing ω_k estimated in the model with the empirical standard deviation of the EBEs [30]. The η -shrinkage is defined as

$$sh_\eta = 1 - \frac{SD(\boldsymbol{\eta}_{EBE}^k)}{\omega_k} \quad (2.24)$$

where sh_η is the η -shrinkage, $SD(\boldsymbol{\eta}_{EBE}^k)$ is the standard deviation of the EBEs for the specific random effects parameter k , and ω_k is the parameter estimated standard deviation [29]. A low η -shrinkage ($SD(\boldsymbol{\eta}_{EBE}^k) \approx \omega_k$) is an indication that the EBEs has been sampled from the assumed distribution. On the other hand, if $sh_\eta > 0.2 - 0.3$ it means that the EBEs has been sampled from a distribution with a relatively smaller standard deviation (hence the term "shrinkage", since the distribution has shrunk in size), and we cannot assume that the EBEs has been sampled from the correct distribution. Negative values of the η -shrinkage are also possible ($SD(\boldsymbol{\eta}_{EBE}^k) > \omega_k$) and occur typically with rich data with small number of subjects, and are a useful signal for possible model mis-specifications [29]. For an example of a model with low η -shrinkage, see Fig. 2.4A.

The second validation tool investigates if there exists a dependency between the EBEs and the individual covariates \mathbf{Z}_i , thus if all elements in $\boldsymbol{\eta}_{EBE}^k$ truly are sampled from a normal distribution with zero mean. This can be visualised by plotting the empirical distribution of the EBEs as box plots, stratified based on each covariate [30]. If no dependency exist all box plots should be centred around zero. However, if there is a dependency there should be a variation in position and spread for boxplots corresponding to different values of a covariate. This can be used as an indication that a dependency with respect to the covariates needs to be added to the model [30]. As an example, the clearance of a drug may be dependent on body weight, where those with high body weight have a larger clearance than those with low body weight. If this dependency is not considered in the PK model, the EBEs for the individuals with high body weight will mainly be positive, while the EBEs for the individuals with low body weight will mainly be negative as compensation. For an example of a model without covariate dependency, see Fig. 2.4B.

The third and last validation tool examines if there exist unspecified correlations between EBEs, in this case between $\boldsymbol{\eta}_{EBE}^1$ and $\boldsymbol{\eta}_{EBE}^2$, in the random effects covariance matrix $\boldsymbol{\Omega}$ (Eq. 2.12). The assumption of no correlation between EBEs can be checked by calculating the sample correlation coefficient between the EBEs, as well as visualise the EBEs in a scatter-plot with the different random effect parameters on each axis, respectively. If the correlation number is high and a trend in the scatter plot is seen, the random effects are probably correlated. The problem with correlation can be handled by adding and estimating the correlation term in the random effects matrix, but only if the data is informative enough to estimate more parameters. If not, this should be interpreted as an

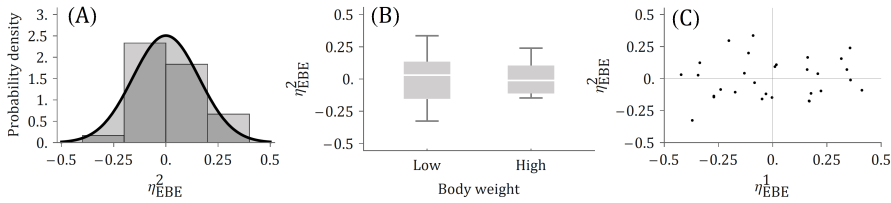


Figure 2.4: (A) Normal distribution $\mathcal{N}(0, \omega_2^2)$ plotted together with the histogram of the sampled EBEs η_{EBE}^2 . The estimated and empirical distribution of the EBEs correspond well with each other, which yields a value of the η -shrinkage of approximately 0.01. (B) The empirical distribution of η_{EBE}^2 visualised as box plots, stratified by body weight. Both box plots centres around zero, indicating that there is no bias. (C) Scatter plot showing the EBEs for each random effects parameter in the model. A small but negligible trend is seen between η_{EBE}^1 and η_{EBE}^2 , and the sample correlation coefficient is 0.12.

indication of problems in model parametrisation, such as overparametrisation or non-identifiability of model parameters [30]. For an example of a model without correlation, see Fig. 2.4C.

2.4.2 Visual Predictive Checks

Visual predictive checks (VPC) is a tool for testing if the chosen NLME model can reproduce the original data used when constructing the model, with respect to both the general trend and the variability in data. The most popular version of VPC is the confidence interval VPC, which is described here, although other versions exist as well [30]. The confidence interval VPC is constructed by, firstly, simulating data from the model using the same study design as the original data (1000 simulated data sets was for example used in [31]). From this large number of data sets user-defined percentiles are calculated, typically the 10th, 50th (median), and 90th percentile [30]. Lastly, for each percentile a nonparametric confidence interval is calculated as a measure of variability of the percentiles [31]. Finally, the model predicted percentiles and corresponding confidence intervals are plotted together with the original data, see Fig 2.5. If a systematic deviation from the original data is seen it could be due to mis-specifications in either the underlying PK/PD model, the observation error model, the covariates model, or the implementation of inter-individual variability. Most importantly, a VPC is easily interpreted in comparison to other more specific graphical tools, such as EBE based diagnostics.

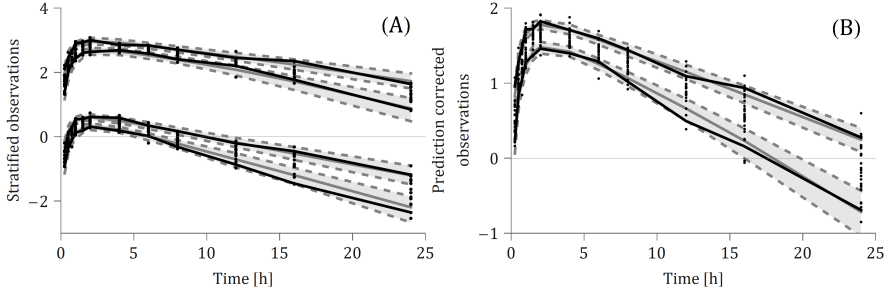


Figure 2.5: Confidence interval visual predictive check (VPC) for a PK model with two different dose groups. The black dots are the original observations, the solid lines are the 10th and 90th percentile of the original observations (black) and model predicted observations (grey), and the shaded grey areas correspond to the 95% confidence interval for each predicted percentile. The data has either been stratified (A), or prediction corrected (B), and the drug concentrations are shown on a logarithmic scale.

Although VPCs is a good tool for evaluating the overall model performance, a common problem is the handling of heterogeneous study designs due to independent variables such as dosing regimens or covariates. One solution is to stratify the data based on these independent variables, such that one VPC for each group of individuals corresponding to the same value of the independent variables is created, see Fig. 2.5A. This method is useful if the data set is rich, meaning that although the data set is divided into smaller parts, each part can still sufficiently represent the data as a whole. However, if the data is sparse such that you are losing information about the population as a whole if stratifying the data, a more suitable option is the prediction correction VPC. In prediction correction VPCs the measurements are weighted based on the independent variables, to retrieve prediction corrected measurements that are more homogeneous. Prediction correction for every individual $i = 1, 2, \dots, N$ and sampling time point $j = 1, 2, \dots, n_i$ is done through the equation

$$pcY_{ij} = lb_{ij} + (Y_{ij} - lb_{ij}) \frac{\widetilde{PRED}_{bin} - lb_{ij}}{PRED_{ij} - lb_{ij}} \quad (2.25)$$

where pcY_{ij} is the prediction corrected observation, Y_{ij} is the observation, lb_{ij} is the lower bound (often set to zero), $PRED_{ij}$ is the population model prediction (the solution to the underlying system of ODEs in a NLME model without inter-individual variability), and \widetilde{PRED}_{bin} is the population model prediction for the median independent variables in a specific bin (where a bin is either a specific sampling time point or a time interval) [31]. Both the original and

simulated data are prediction corrected using the population model predictions according to Eq. (2.25), and the resulting VPC plot is shown in Fig. 2.5B. In this particular example the lower bound would equal zero, the measurements for all individuals are taken at the same sampling time points ($n_i = n$, thus no need for binning), and we have to correct for the two dose groups (small *versus* large drug dose). Therefore, the prediction correction of the last measurement ($t=24h$) for an individual i that got a small drug dose becomes

$$pcY_{in} = Y_{in} \frac{\widetilde{PRED}_n}{PRED_{in}} \quad (2.26)$$

where $PRED_{in}$ is the population model prediction for all individuals who got the small drug dose, while \widetilde{PRED}_n is the population model prediction for the median drug dose at sampling time point n (Fig. 2.5).

2.5 Optimal Design

In previous sections it has been discussed how to develop, estimate, and evaluate a PK/PD model using the NLME framework, but little attention has been given to what these models are actually based upon - the data. The data of consideration (drug concentration, biomarker response, heart rate etc.) are also an important aspect of the model building process, since if the data are not informative it will be much more difficult to extract the key characteristics from the biological system of consideration. Therefore, this last section will give some well-deserved attention to optimal design; how to use mathematical modelling to design protocols or experiments to retrieve as informative data as possible (Fig. 2.6).

The essential basis for the optimised planning of an experiment is provided by the Cramér-Rao inequality. The Cramér-Rao inequality states that the variance-covariance matrix of any unbiased estimator is bounded by the inverse of the Fisher information matrix

$$Cov(\mathbf{q}, \mathcal{D}, \Theta) \geq \mathcal{I}(\mathbf{q}, \Theta)^{-1} \quad (2.27)$$

or, equivalently, that the difference between the variance-covariance matrix and the Fisher information matrix ($Cov(\mathbf{q}, \mathcal{D}, \Theta) - \mathcal{I}(\mathbf{q}, \Theta)^{-1}$) is positive-semidefinite [3, 32, 33, 34]. Here Θ denote the collection of model parameters

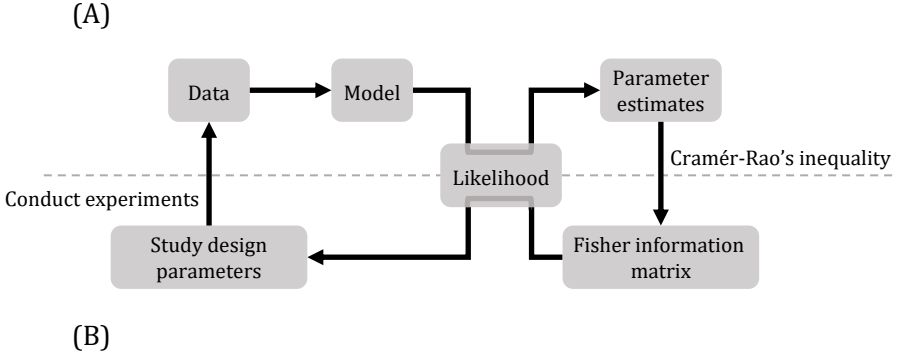


Figure 2.6: The complete circle of modelling. (A) The model building process starting with creating a model based on characteristics seen in data, then using a parameter estimation procedure, dependent of the likelihood, to obtain the optimal model parameters. (B) The optimal design process where the Fisher information matrix, also dependent of the likelihood, is calculated based on the model with its optimal parameter values. From this, the optimal design variables can be obtained, that in turn can be used to produce even more informative data.

$\{\theta, \Omega, \Sigma\}$, \mathcal{D} the observations, and \mathbf{q} the design specific variables. Specifically, \mathbf{q} is a collection of different study design related variables such as the sampling schedule, the number of sampling time points, the dose levels, or the number of test subjects. The Fisher information matrix is a measure of the amount of information the observations \mathcal{D} carries about the model parameters Θ and is defined as

$$\mathcal{I}(\mathbf{q}, \Theta) = -\mathbb{E}_{\mathcal{D}} \left[\frac{\partial}{\partial \Theta} \log \mathcal{L}(\Theta|\mathcal{D}) \frac{\partial}{\partial \Theta} \log \mathcal{L}(\Theta|\mathcal{D})^T \right] \quad (2.28)$$

where $\mathcal{L}(\Theta|\mathcal{D}) = \mathcal{L}(\theta, \Sigma, \Omega|\mathcal{D})$ is the likelihood function defined in Equation (2.15). In this setting however, compared to section 2.3, the parameters in Θ are assumed to be fixed to their optimal values, and the variables in \mathbf{q} are the ones being estimated (Fig 2.6) [32].

The goal in optimal design is to find the study design variables \mathbf{q} that gives the highest information content in data, quantified in terms of the Fisher information matrix. In practice, the size of the Fisher information matrix is measured in terms of a scalar function called *design criterion* that maps the matrix to a scalar number, such that comparisons of Fisher information matrices are plausible. Several design criteria exist that quantifies the size of the matrix

differently, but one of the most common design criteria is the D-optimality or lnD-optimality [32]. D-optimality maximises the determinant of the matrix and is defined as

$$\mathbf{q}_D^* = \underset{\mathbf{q}}{\operatorname{argmax}} \det \mathcal{I}(\mathbf{q}, \Theta) \quad (2.29)$$

where \mathbf{q}_D^* is the optimal study design variables and $\det \mathcal{I}(\mathbf{q}, \Theta)$ is the objective function for this specific design criterion. To get lnD-optimality, one takes the logarithm of the determinant of the Fisher information matrix which provides higher numerical stability while leaving the optima unaffected [32]. For a complete list of different design criteria, see [35].

2.5.1 Design Optimisation Procedure

Since the optimisation problem is often multi-dimensional and the objective function is often non-smooth and non-linear, optimisation of experimental design is not a trivial task. In addition, simultaneous optimisation of several different study design variables has been shown to out-perform sequential optimisation of each study design variable at a time [33], meaning that the optimisation method needs to be able to handle several different types of design variables, such as continuous drug dose ranges or discrete sample time points. To retrieve the results for Paper II the software PopED has been used for optimisation of design, and the default asymptotically global optimisation technique for the software will be described further. However, as a limitation only the optimisation procedure for retrieving the optimal sampling schedule and continuous variables, such as dose levels, will be discussed. For a complete list, see [3, 32].

The optimisation procedure starts with defining start guesses and boundaries for each study design variable that must be feasible and realistic. For example, the initial and maximum number of measurements must be defined prior to the estimation, since the obvious solution would otherwise be to have an infinite number of measurements, which is not realistic. The next step is then to give the study design variables and corresponding boundaries, together with appropriate software settings, as input to the algorithm.

The algorithm consists of three separate steps: 1) an adaptive random search (ARS), 2) a Broyden–Fletcher–Goldfarb–Shanno (BFGS, described in section 2.3) algorithm, and 3) a line search (LS) [32]. Starting with the ARS, it is an iterative global optimisation method that does not require any calculation of

the derivative of the objective function. Let OF denote the objective function, independent of choice of design criteria, and the continuous experimental variables such as the sampling schedule and dose levels be denoted \mathbf{e} . Then the ARS at iteration $k + 1$ can be defined as [3]:

$$\mathbf{e}_{k+1} = \begin{cases} \mathbf{e}_k, & \text{if } OF(\mathbf{e}_k + \Delta\mathbf{e}_k) < OF(\mathbf{e}_k) \\ \mathbf{e}_k + \Delta\mathbf{e}_k, & \text{if } OF(\mathbf{e}_k + \Delta\mathbf{e}_k) \geq OF(\mathbf{e}_k) \end{cases} \quad (2.30)$$

$$\Delta\mathbf{e}_k \sim \mathcal{N}(0, \mathbf{S})$$

Here \mathbf{S} is the locality of the random search, defined as a matrix with diagonal elements equal to the distance between the upper and lower bound for the specific study design variable in \mathbf{e} , divided by a locality factor s [3]. In the beginning s takes a small value, allowing a search over the whole admissible domain of the variables, but if the current objective function value remains unchanged after a certain number of iterations s starts to successively increase. In this way the neighbourhood at the present optimum is narrowed such that the result can be refined, hence an *adaptive* random search [3, 36]. Lastly, if $\mathbf{e}_k + \Delta\mathbf{e}_k$ at one iteration is not in the admissible domain it will take the value at the boundary instead [3]. For example, if the maximal dose level is exceeded given the current step size, the choice in Eq. (2.30) would be to either stay at the current dose level or change to the maximal dose level, whatever increases the objective function value.

The line search in this context should not be confused with the procedure of consecutively finding the appropriate step size in the descent direction, which is a more common definition of line search [37]. Here, the LS algorithm sequentially performs a search in each dimension of the design, for example each sampling time point or dose level, while keeping the remaining design variables fix to its current optimum [32, 36]. The admissible domain for each study design variable is discretized given an either default or user-defined number of grid points, and the algorithm checks if a change in each and every study design variable could increase the objective function value.

Lastly, to compare the performance of a study design relative a reference design, D-efficiency is used. D-efficiency is calculated as

$$D_{eff} = \left(\frac{\det \mathcal{I}(\mathbf{q}^*, \Theta)}{\det \mathcal{I}(\mathbf{q}, \Theta)} \right)^{1/P} \quad (2.31)$$

where \mathbf{q}^* is the current optimal study design variables, \mathbf{q} are the study design variables from the previous iteration (or the initial guess for the first iteration), and P is the number of model parameters. If the study design variables has barely changed between two iterations (typically $D_{eff} \leq 1.001$), the algorithm stops [32]. Otherwise it runs through the methods again and calculates the D-efficiency until convergence (Fig. 2.7).

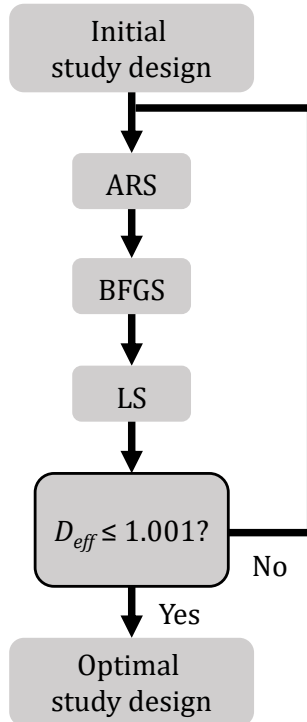


Figure 2.7: Schematic illustration of the default optimisation technique used in PopED. The start guesses and boundaries of the study design variables \mathbf{q} first enters the adaptive random search (ARS) and leaves the ARS when either the maximum number of iterations is reached or when the objective function value has not changed after a certain number of iterations. The result from the ARS then enters the Broyden–Fletcher–Goldfarb–Shanno (BFGS) algorithm and leaves when convergence is reached. The result from the BFGS algorithm then enters the line search (LS) and leaves when the LS has gone through every study design variable. Lastly, the D-efficiency is calculated to check if the current optimal study design variables \mathbf{q}^* have changed notably relative \mathbf{q} . If not the algorithm stops, and otherwise it runs through the methods again, starting at the ARS.

3 Summary of Papers

Paper I: Second-generation TNF α turnover model for improved analysis of test compound interventions in LPS challenge studies

This work presents a turnover model describing TNF α release after LPS provocations in absence or presence of anti-inflammatory test compounds, using NLME modelling. We have constructed a mathematical framework able to capture both detailed characteristics and general trends, using an extensive data set together with an extended version of a previously published challenge model from our team. The goal has been to develop a framework capable of modelling TNF α response in LPS challenge studies *in vivo* and demonstrate its general applicability in model informed drug development for different types of test compounds and despite inter-occasion variability. What makes our work stand out from previously published models is the thorough investigation of the LPS-induced stimulation of TNF α response and in turn how it influences the estimated pharmacological effects, as well as the inclusion of inter-individual variability through NLME modelling.

For a drug discovery setting, the suggested framework characterises the different sources of variability that is often observed in biomarker responses after LPS challenge, and enables estimation of pharmacodynamic parameters (mainly I_{max} and IC_{50} values) with good precision. Moreover, the flexible handling of different study designs allows for pooling of data from very different experimental formats: data from studies with multiple doses of challenger, multiple doses of test compounds, or different test compounds (including reference drugs used as positive controls) can be analysed simultaneously. This extraction and utilisation of data from different sources also helps reduce the number of animals per study, which is very important for animal welfare reasons and in a drug discovery setting in general.

Paper II: Optimizing study design in LPS challenge studies for quantifying drug induced inhibition of TNF α response: Did we miss the prime time?

This work uses the model created in Paper I for improvement of the experimental design in pre-clinical *in vivo* LPS challenge studies. Since TNF α response data from LPS challenge studies are very rapid and transient, the data at hand must be informative to distinguish the key characteristics (such as the inhibiting effect of the test compound) from the variability in data. In this work, we provide general guidelines of how to optimize the study design for quantification of drug induced inhibition of TNF α response in LPS challenge studies, as well as a summary of how people have conducted these kinds of experiments in the past.

The study design variables of special interest are the time difference between LPS and test compound dosing, sampling time points, and initial LPS dose. To investigate if a more effective inhibition of TNF α response can be achieved by altering the time difference between system inputs, synthetic data has been generated by simulation and compared statistically to see if one can observe a difference in response despite the variability in response. For the remaining study design related variables the software tool PopED for optimal design, together with the suggested model from Paper I, has been used to find the study design variables that maximises the amount of information in data. In parallel with the optimisation of experimental design, a literature study has been conducted summarising how LPS challenge studies have been conducted in the past, giving a broader perspective of how LPS challenge studies are usually conducted both in a pre-clinical and clinical setting. By using the recommendations provided in this study the information retrieved from an initial small pilot study should create sufficient insight to become a robust basis for designing future pre-clinical and clinical studies and trials, respectively.

Paper III: NLMEModeling: A Wolfram Mathematica Package for Nonlinear Mixed Effects Modeling of Dynamical Systems

In this work we present the latest version of the Mathematica package `NLMEModeling` developed at FCC, used for parameter estimation of non-linear mixed effects models described by either ordinary or stochastic differential equations. The original purpose behind the code base now denoted `NLMEModeling` was to provide an efficient proving ground for algorithm development addressing short comings identified in how gradient based optimisation in state-of-the-art NLME software was performed, leading to the sensitivity based FOCE method or S-FOCE [26, 28]. In addition, there has been an increasing interest in extending the NLME framework to incorporate stochastic differential equations, but the software options available for this class of models were limited. Furthermore, Wolfram Mathematica was found to be a suitable platform for NLME modelling [38], but no current functionality for estimation of NLME models existed.

The implemented parameter estimation procedure uses this first-order conditional estimation (FOCE) method to approximate the likelihood function, and a gradient-based optimisation method called Broyden-Fletcher-Goldfarb-Shanno (BFGS) algorithm to find the optimal fixed and random effects. In addition, sensitivity equation-based gradients of the objective function is used instead of finite differences. For SDEs, the extended Kalman filter is used for calculating the expected observation values and the corresponding covariance matrix given data, and the Euler-Maruyama discretisation is used for simulation of the stochastic differential equations.

In addition to the parameter estimation techniques, several tools are available for evaluating the result as well as comparing the result with competing models. Goodness-of-fit plots, diagnostic plots based on the empirical Bayes estimates (EBEs), and pcVPCs are some examples of the built-in functions for model evaluation available in the package. In addition, if further evaluation is required all information concerning the estimation result is provided in the model object. In summary, `NLMEModeling` is a user-friendly environment for estimation and evaluation of non-linear mixed effects models, where the extension from ODEs to SDEs is seamless.

4 Outlook

In this thesis $\text{TNF}\alpha$ response from pre-clinical LPS challenge studies has been studied in detail, both how to construct a model describing the response as well as optimise the study design to retrieve more informative data. In addition, a software package `NLMEModeling` has been developed to aid in the model estimation and evaluation process. Even though several contributions have been made to the research community, there are always refinements to be done. After all, modelling is an iterative process. This chapter highlights some of the improvements that could be made to develop these pieces of research further.

While several models of $\text{TNF}\alpha$ response in pre-clinical LPS challenge studies exist [6, 7, 15, 39, 40, 41], the amount of data used for constructing the model in Paper I is much larger than for the previous models, to the authors best knowledge. It would therefore be interesting to make an unbiased comparison of models on new data to explore the different models' strengths and weaknesses. For example: Is it possible to fit the model in Paper I to a sparser data set and still retrieve parameter estimates with acceptable precision? Is the simplistic model presented in [7] sufficient for the describing the complex $\text{TNF}\alpha$ response? And would a model derived from the biological mechanisms fit data as good as models using the more classical PK/PD approach [41]? Answering these questions as well as comparing similarities and differences between the models would help summarising the field of $\text{TNF}\alpha$ response models, which in turn could lead to better understanding of the reliability of the pharmacodynamic effect derived from the models.

The comparison of different models on new data would be a part of the model validation process, where validation of a model is almost as important as the model building process itself. As an additional part of the validation step, it would be interesting to conduct new LPS challenge experiments based on the optimal design proposed in Paper II. This would not only validate the usefulness of optimal design for $\text{TNF}\alpha$ response in LPS challenge studies but also the model derived in Paper I. Since one of the goals in optimal design is

to minimise the uncertainty in model parameters, it requires that the chosen model sufficiently represents data. Using the same reasoning as for the model comparison, it would be equally interesting to check what the optimal design would be if using other already existing models for $\text{TNF}\alpha$ response in LPS challenge studies. Lastly, it would be of interest to optimise more study design parameters, such as the number of sample time points, for further refinement of the results.

Looking even further, during the course of work resulting in Paper II it was clear that $\text{TNF}\alpha$ response in clinical studies share similar dynamics as the response in pre-clinical studies. The translation from pre-clinical to clinical LPS challenge studies has proven to be difficult [42, 43], and it seems there exist a need for useful tools to facilitate the translation from animals to humans. If the existing $\text{TNF}\alpha$ turnover model could be extended to consider inter-species scaling, and find an optimal design that suits all species, the results from the clinical studies could be improved.

To this end the $\text{TNF}\alpha$ response model has been defined as an ODE based NLME model, but an additional extension could be to model the $\text{TNF}\alpha$ response using stochastic differential equations (SDEs). The major problem with $\text{TNF}\alpha$ response in LPS challenge studies has been shown to be the variability in response, and describing the variability in data with inter-individual variability, observation error *and* stochasticity in the system dynamics would potentially reduce the observation further, compared to the NLME model, as well as increase the precision in the estimated parameters. Defining the different sources of variability in response could help understand the underlying biology, as well as help pinpoint areas in need for improvement of the model.

Moving from ODEs to SDEs would be seamless if using `NLMEModeling` in terms of parameter estimation, but more needs to be done concerning SDE model evaluation. There are currently no evaluation tools that solemnly checks if the stochasticity is implemented correctly in `NLMEModeling`. Many of the available model evaluation tools are not designed to handle the stochasticity in SDEs, for example the `pcVPC`. Continuing on the topic of VPCs, a common trait that has not yet been added to the `NLMEModeling` package is binning. As mentioned in section 2.4.2, a bin is either a specific sampling time point or a time interval, where only the former is currently implemented in `NLMEModeling`. Lastly, many of the model evaluation tools should be developed to be more flexible, to be able to handle the larger variety of models and corresponding data that is emerging.

In conclusion, although the appended papers serve as a good contribution to the research community more work can still be done in the field of $\text{TNF}\alpha$ response in LPS challenge studies in particular, and in the field of parameter estimation and model evaluation in general. This in turn means that there is much more to learn about LPS challenge studies which, maybe luckily, means Hell itself won't open as Lewis Thomas proposed [44]. At least just not yet.

Bibliography

- [1] J. Gabrielsson and D. Weiner. *Pharmacokinetic and pharmacodynamic data analysis: concepts and applications*. CRC press, 5th edition, 2001. ISBN 978-91-982991-0-6.
- [2] D. Mager, E. Wyska, and W. Jusko. Diversity of mechanism-based pharmacodynamic models. *Drug Metabolism and Disposition*, 31(5):510–518, 2003. doi: 10.1124/dmd.31.5.510.
- [3] M. Foracchia, A. Hooker, P. Vicini, and A. Ruggeri. POPED, a software for optimal experiment design in population kinetics. *Computer Methods and Programs in Biomedicine*, 74(1):29–46, 2004. doi: 10.1016/S0169-2607(03)00073-7.
- [4] R. Lalonde, K. Kowalski, M. Hutmacher, W. Ewy, D. Nichols, P. Milligan, B. Corrigan, P. Lockwood, S. Marshall, L. Benincosa, T. Tensfeldt, K. Parivar, M. Amantea, P. Glue, H. Koide, and R. Miller. Model-based drug development. *Clinical Pharmacology & Therapeutics*, 82(1):21–32, 2007. doi: 10.1038/sj.clpt.6100235.
- [5] B. Alberts, A. Johnson, J. Lewis, D. Morgan, M. Raff, K. Roberts, and P. Walter. *Molecular biology of the cell*. Garland Science, New York, 6th edition, 2015. ISBN 978-0-8153-4464-3.
- [6] A. Chakraborty, S. Yeung, N. Pyszczynski, and W. Jusko. Pharmacodynamic interactions between recombinant mouse interleukin-10 and prednisolone using a mouse endotoxemia model. *Journal of Pharmaceutical Sciences*, 94(3):590–603, 2005. doi: 10.1002/jps.20257.
- [7] P. Gozzi, I. Pählman, L. Palmér, A. Grönberg, and S. Persson. Pharmacokinetic-pharmacodynamic modeling of the immunomodulating agent susalimod and experimentally induced tumor necrosis factor- α levels in the mouse. *Journal of Pharmacology and Experimental Therapeutics*, 291(1):199–203, 1999.

- [8] Q. Wang, Y. Zhang, P. Hall, L. Lin, U. Raut, N. Mollova, N. Green, J. Cuzzo, S. Chesley, X. Xu, J. Levin, and V. Patel. A rat pharmacokinetic/pharmacodynamic model for assessment of lipopolysaccharide-induced tumor necrosis factor- α production. *Journal of Pharmacological and Toxicological Methods*, 56(1):67–71, 2007. doi: 10.1016/j.vascn.2007.02.001.
- [9] F. Held, E. Hoppe, M. Cvijovic, M. Jirstrand, and J. Gabrielsson. Challenge model of TNF α turnover at varying LPS and drug provocations. *Journal of Pharmacokinetics and Pharmacodynamics*, 46(3):223–240, 2019. doi: 10.1007/s10928-019-09622-x.
- [10] D. Anderson. *Compartmental modeling and tracer kinetics*, volume 50. Springer Science & Business Media, 2013. ISBN 978-3-642-51861-4.
- [11] W. Jusko. Moving from basic toward systems pharmacodynamic models. *Journal of pharmaceutical sciences*, 102(9):2930–2940, 2013. doi: 10.1002/jps.23590.
- [12] I. Irurzun-Arana, C. Rackauckas, T. McDonald, and I. Trocóniz. Beyond deterministic models in drug discovery and development. *Trends in Pharmacological Sciences*, 41:1–14, 2020. doi: 10.1016/j.tips.2020.09.005.
- [13] D. Mould and R. Upton. Basic concepts in population modeling, simulation, and model-based drug development. *CPT: pharmacometrics & systems pharmacology*, 1(9):1–14, 2012. doi: 10.1038/psp.2012.4.
- [14] P. Macheras and A. Iliadis. *Deterministic Compartmental Models*. In: *Modeling in Biopharmaceutics, Pharmacokinetics and Pharmacodynamics: Homogeneous and Heterogeneous Approaches*, volume 30, pages 191–210. Springer International Publishing, Cham, 2016. doi: 10.1007/978-3-319-27598-7_8.
- [15] J. Gabrielsson, S. Hjorth, B. Vogg, S. Harlfinger, P. Morentin Gutierrez, L. Peletier, R. Pehrson, and P. Davidsson. Modeling and design of challenge tests: Inflammatory and metabolic biomarker study examples. *European Journal of Pharmaceutical Sciences*, 67:144–159, 2015. doi: 10.1016/j.ejps.2014.11.006.
- [16] D. van Lier, C. Geven, G. Leijte, and P. Pickkers. Experimental human endotoxemia as a model of systemic inflammation. *Biochimie*, 159:99–106, 2019. doi: 10.1016/j.biochi.2018.06.014.
- [17] D. Brooks, L. Barr, S. Wiscombe, D. McAuley, J. Simpson, and A. Rostron. Human lipopolysaccharide models provide mechanistic and therapeutic insights into systemic and pulmonary inflammation. *European Respiratory Journal*, 56(1), 2020. doi: 10.1183/13993003.01298-2019.

- [18] R. Savic, D. Jonker, T. Kerbusch, and M. Karlsson. Implementation of a transit compartment model for describing drug absorption in pharmacokinetic studies. *Journal of pharmacokinetics and pharmacodynamics*, 34(5):711–726, 2007. doi: 10.1007/s10928-007-9066-0.
- [19] M. Lindstrom and D. Bates. Nonlinear mixed effects models for repeated measures data. *Biometrics*, 46:673–687, 1990. doi: 10.2307/2532087.
- [20] Monolix. Residual error model [internet]. <https://monolix.lixoft.com/data-and-models/errormodel/>, cited 210509.
- [21] S. Laporte-Simitsidis, P. Girard, P. Mismetti, S. Chabaud, H. Decousus, and J. Boissel. Inter-study variability in population pharmacokinetic meta-analysis: when and how to estimate it? *Journal of pharmaceutical sciences*, 89(2):155–167, 2000. doi: 10.1002/(SICI)1520-6017(200002)89:2<155::AID-JPS3>3.0.CO;2-2.
- [22] Y. Wang. Derivation of various NONMEM estimation methods. *Journal of Pharmacokinetics and pharmacodynamics*, 34(5):575–593, 2007. doi: 10.1007/s10928-007-9060-6.
- [23] E. Kuhn and M. Lavielle. Maximum likelihood estimation in nonlinear mixed effects models. *Computational statistics & data analysis*, 49(4):1020–1038, 2005. doi: 10.1016/j.csda.2004.07.002.
- [24] J. Leander, J. Almquist, A. Johnning, J. Larsson, and M. Jirstrand. NLMEM-odeling: A Wolfram Mathematica package for nonlinear mixed effects modeling of dynamical systems. *arXiv preprint: arXiv:2011.06879 [stat.CO]*, 2020.
- [25] E. Vonesch. A note on the use of Laplace’s approximation for nonlinear mixed-effects models. *Biometrika*, 83(2):447–452, 1996. doi: 10.1093/biomet/83.2.447.
- [26] J. Almquist, J. Leander, and M. Jirstrand. Using sensitivity equations for computing gradients of the FOCE and FOCEI approximations to the population likelihood. *Journal of pharmacokinetics and pharmacodynamics*, 42(3):191–209, 2015. doi: 10.1007/s10928-015-9409-1.
- [27] J. Nocedal and S. Wright. *Numerical Optimization*. Springer-Verlag, New York, 2006. doi: 10.1007/978-0-387-40065-5.
- [28] H. Olafsdottir, J. Leander, J. Almquist, and M. Jirstrand. Exact gradients improve parameter estimation in nonlinear mixed effects models with stochastic dynamics. *AAPS journal*, 20(5):1–13, 2018. doi: 10.1208/s12248-018-0232-7.

- [29] R. Savic and M. Karlsson. Importance of shrinkage in empirical Bayes estimates for diagnostics: Problems and solutions. *AAPS journal*, 11: 558–569, 2009. doi: 10.1208/s12248-009-9133-0.
- [30] T. Nguyen, M. Mouksassi, N. Holford, N. Al-Huniti, I. Freedman, A. Hooker, J. John, M. Karlsson, D. Mould, J. Pérez Ruixo, E. Plan, R Savic, J. van Hasselt, B. Weber, C. Zhou, E. Comets, F. Mentré, and for the Model Evaluation Group of the International Society of Pharmacometrics (ISoP) Best Practice Committee. Model evaluation of continuous data pharmacometric models: Metrics and graphics. *CPT: Pharmacometrics & Systems Pharmacology*, 6(2):87–109, 2017. doi: 10.1002/psp4.12161.
- [31] M. Bergstrand, A. Hooker, J. Wallin, and M. Karlsson. Prediction-corrected visual predictive checks for diagnosing nonlinear mixed-effects models. *AAPS journal*, 13:143–151, 2011. doi: 10.1208/s12248-011-9255-z.
- [32] J. Nyberg, S. Ueckert, E. Strömberg, S. Hennig, M. Karlsson, and A. Hooker. PopED: An extended, parallelized, nonlinear mixed effects models optimal design tool. *Computer Methods and Programs in Biomedicine*, 108(2): 789–805, 2012. doi: 10.1016/j.cmpb.2012.05.005.
- [33] J. Nyberg, M. Karlsson, and A. Hooker. Simultaneous optimal experimental design on dose and sample times. *Journal of pharmacokinetics and pharmacodynamics*, 36(2):125, 2009. doi: 10.1007/s10928-009-9114-z.
- [34] E. Strömberg and A. Hooker. The effect of using a robust optimality criterion in model based adaptive optimization. *Journal of pharmacokinetics and pharmacodynamics*, 44(4):317–324, 2017. doi: 10.1007/s10928-017-9521-5.
- [35] A. Atkinson and A. Donev. *Optimum experimental designs*. Oxford University press, 1992. ISBN 0-19-852254-1.
- [36] A. Hooker, M. Forrachia, E. Strömberg, M. Fink, G. Lestini, S. Ueckert, and J. Nyberg. Package ‘PopED’ [internet]. <https://cran.r-project.org/web/packages/PopED/PopED.pdf>, 2021.
- [37] N. Andréasson, A. Evgrafov, E. Gustavsson, Z. Nedělková, M. Patriksson, K.C. Sou, and M. Önnheim. *An Introduction to Continuous Optimization*. Studentlitteratur, 3rd edition, 2016.
- [38] Wolfram Research, Inc. *Mathematica*, Version 12.3.1 [internet]. <https://www.wolfram.com/mathematica>. Champaign, IL, 2021.
- [39] E. Wyska. Pharmacokinetic-pharmacodynamic modeling of methylxanthine derivatives in mice challenged with high-dose lipopolysaccharide. *Pharmacology*, 85:264–271, 2010. doi: 10.1159/000288734.

- [40] A. Thorsted, S. Bouchene, E. Tano, M. Castegren, M. Lipcsey, J. Sjölin, M. Karlsson, L. Friberg, and E. Nielsen. A non-linear mixed effect model for innate immune response: *In vivo* kinetics of endotoxin and its induction of the cytokines tumor necrosis factor alpha and interleukin-6. *PloS one*, 14(2):e0211981, 2019. doi: 10.1371/journal.pone.0211981.
- [41] E. Nyman, M. Lindh, W. Lövfors, C. Simonsson, A. Persson, D. Eklund, E. Bäckström, M. Fridén, and G. Cedersund. Mechanisms of a sustained anti-inflammatory drug response in alveolar macrophages unraveled with mathematical modeling. *CPT: pharmacometrics & systems pharmacology*, 9(12):707–717, 2020. doi: 10.1002/psp4.12568.
- [42] M. Fink. Animal models of sepsis. *Virulence*, 5(1):143–153, 2014. doi: 10.4161/viru.26083.
- [43] C. Shu, H. Zhou, M. Afsharvand, L. Duan, H. Zhang, R. Noveck, and D. Raible. Pharmacokinetic-pharmacodynamic modeling of apratastat: A population-based approach. *The Journal of Clinical Pharmacology*, 51(4): 472–481, 2011. doi: 10.1177/0091270010372389.
- [44] K. Brigham, editor. *Endotoxin and the lungs*, volume 77. Marcel Dekker Inc., New York, 1994. ISBN 0-8247-9222-X.

